International Journal of Engineering Science 217 (2025) 104356

Contents lists available at ScienceDirect

International Journal of Engineering Science

journal homepage: www.elsevier.com/locate/ijengsci

Full length article

Effect of surface stresses on pull-in instability of a nanocantilever under electrostatic and intermolecular forces

Gennadi I. Mikhasev [a], Enrico Radi [b,*]

[a] Department of Astronautical Science and Mechanics, Harbin Institute of Technology, P.O. Box 301, 92 West Dazhi Street, 150001 Harbin, China

[b] Dipartimento di Scienze e Metodi dell'Ingegneria, Università di Modena e Reggio Emilia, Via Amendola 2, 42122 Reggio Emilia, Italy

ARTICLE INFO

Keywords:
Nanocantilever
Electrostatic and intermolecular forces
Surface stresses
Pull-in instability
Self-buckling

ABSTRACT

The problem of pull-in instability of an electrostatically actuated nanocantilever is investigated here by considering the effect of the residual surface stress and surface attractions. A novel approach is developed by replacing the original differential equation with an equivalent integral equation for the deflection, obtained by using the Green's function of the nanocantilever. Moreover, the resultant lateral force is approximated by a power function of the axial coordinate containing two unknown parameters, namely the power-law exponent and the tip deflection. These two unknowns can be found from a matching procedure by requiring that the approximated distribution of the lateral force calculated at the midspan and at the free tip must coincide with the actual load distribution calculated from the deflection predicted by the governing integral equation when the approximated load distribution is considered. In this way, a system of two nonlinear algebraic equations for the two unknown parameters as functions of the applied voltage is derived. The maximum attained by the electrostatic voltage then provides the approximated values of the pull-in voltage and the pull-in deflection. The plotted results show the effects of positive and negative residual surface stress and surface attractions on the pull-in parameters. A practical application is also considered for a nanocantilever made of Silicon with crystallographic direction [100] on faces. It is observed that for a very thin Si[100] nanocantilever there exists a critical length at which the nanobeam buckles without any applied electrostatic voltage and for any gap distance between movable and fixed electrodes.

1. Introduction

The effect of surface residual stress is extremely important for the accurate prediction of the pull-in behavior of nanocantilevers because at the nanoscale, surface effects become comparable to or even dominate bulk properties (Altenbach & Eremeyev, 2011; Eremeyev, 2016). Indeed, at the nanoscale, nanobeams have a high surface-to-volume ratio, and thus surface phenomena, including residual stress, significantly influence their mechanical behavior (Cuenot, Fretigny, Demoustier-Champagne, & Nysten, 2004; Zhou & Huang, 2004). Moreover, residual surface stress can modify the bending stiffness of nanobeams by increasing the effective stiffness if it is tensile, and decreasing the effective stiffness if it is compressive (Altenbach & Eremeyev, 2017; Mikhasev, 2025), making it more prone to buckling (Wang & Feng, 2009) or pull-in at lower voltages. This change in bending stiffness directly impacts the pull-in voltage, which is the voltage at which the electrostatic force overcomes the mechanical restoring force, causing collapse. Therefore, predicting pull-in voltage without accounting for surface residual stress can lead to inaccurate results in nanoelectromechanical

* Corresponding author.
E-mail addresses: mikhasev@hit.edu.cn (G.I. Mikhasev), eradi@unimore.it (E. Radi).

https://doi.org/10.1016/j.ijengsci.2025.104356
Received 15 May 2025; Received in revised form 16 July 2025; Accepted 16 July 2025
Available online 15 August 2025

systems (NEMS) design. This inaccuracy is critical in applications like nano-switches, sensors, and actuators, where stability and precise control of pull-in voltage are essential.

The number of papers dealing with the analysis of the surface effects impact on the pull-in instability of electrically actuated micro- and nanosized beams is small. We will not discuss here approaches used in the relevant works, since they are the same as in numerous investigations that do not take into account surface effects (e.g., see in studies Dequesnes, Rotkin, & Aluru, 2002; Mousavi, Bornassi, & Haddadpour, 2013; Ramezani, Alasty, & Akbari, 2007; Soroush et al., 2010; Yang, Jia, & Kitipornchai, 2008 and in the review articles Khaniki, Ghayesh, & Amabili, 2021; Zhang, Yan, Peng, & Meng, 2014), but we will focus on how these effects were considered in a particular paper. Probably, the first study on pull-in instability of the bridge-type microswitch taking into account surface residual stress was carried out by Huang et al. (2001). They proposed a simplified model ignoring surface stresses due to deformations in the bulk, but capturing the residual surface stress by introducing an additional term in the governing equation. The influence of surface stresses, including residual ones, on the pull-in instability of electrostatic beam-like switches and actuators was studied by Duan and Rach (2013), Farrokhabadi, Mohebshahedin, Rach, and Duan (2016) and Ma, Jiang, and Asokanthan (2010) using the classical Euler–Bernoulli beam model. The latter was modified by introducing into the bending stiffness an additional term depending on the surface Young modulus, while the residual surface stresses were taken into account with the standard way, as in Huang et al. (2001). In particular, an equivalent integral equation for a nanocantilever under electrostatic actuation is derived in Duan and Rach (2013) by considering the influence of surface energy. Then, making use of a second-degree polynomial as the shape function of the beam deflection, an analytic expressions is obtained for the tip deflection and pull-in parameters of the nanobeam. However, the influence of the surface energy on the boundary conditions has been ignored by Duan and Rach (2013), thus leading to the questionable result that the effect of surface elasticity decreases the pull-in voltage and deflection. Later, the problem was reformulated by Farrokhabadi et al. (2016) with the correct boundary conditions, and it was found that the surface elasticity increases the pull-in voltage. In other words, the existence of surface energy causes the structure to deflect more stiffly.

Analytical bounds to the pull-in voltage of a nanocantilever under the action of electrostatic, van der Waals and Casimir forces were provided by Radi, Bianchi, and Nobili (2021), by considering also the size effects in the spirit of the surface elasticity theory. The work confirmed that a positive residual stress stabilizes the system by increasing the pull-in voltage. Up to now, no investigations were performed on the effects of a negative residual stress on the pull-in voltage of a nanocantilever. A contribution related to this problem was however given in Radi, Bianchi, and di Ruvo (2018), where the effect of a compressive axial load on the pull-in instability is studied and is found to reduce the pull-in voltage of a nanocantilever significantly. Therefore, if the contribution of a compressive axial load due to negative residual stress is neglected, then the pull-in voltage may be considerably overestimated. This inaccuracy may lead to unexpected damage during service operation.

A modified Euler–Bernoulli model of an electrically actuated nanobeam within the framework of the Gurtin-Murdoch surface elasticity theory (Gurtin & Murdoch, 1975, 1978), was proposed by Fu and Zhang (2011). To satisfy the third equation of the forces balance at the upper and lower surfaces with residual stresses, they introduced an additional hypothesis on the normal stress σ_{33}, which is assumed to be a linear functions of the transverse coordinate z. The same assumption on the linear distribution of the normal stresses σ_{33} in the thickness direction was made by Ansaria, Gholami, Faghih Shojaei, Mohammadia, and Sahmania (2014) adn Ansari, Mohammadi, Faghih Shojaei, Gholami, and Darabi (2014) to investigate the hydrostatically and electrostatically actuated pull-in instability of circular and rectangular nanoplates, taking into account surface stresses including the residual ones. The above contributions convincingly demonstrated the strong influence of surface stresses on the pull-in voltage and deflection. In particular, it was found (Ansari et al., 2014) that the presence of positive residual surface stress results in growing the bending stiffness and later on, the pull-in voltage, while a negative residual surface stress leads to the opposite results, such effect becoming more pronounced under decreasing the beam/plate thickness.

A common feature of the above-mentioned studies on the pull-in instability of micro- and nanosized beams and plates with surface effects is that they are based on kinematic hypotheses within the framework of classical beam and plate theories and, in some cases, contain an additional hypothesis predicting the distribution of normal stresses across the beam/plate thickness. In the recently published paper (Mikhasev, 2025), a novel model for ultrathin plates with surface energy is proposed, which is obtained by direct integration of 3D elasticity equations and is free from any kinematic hypothesis. There, it is shown that introducing an additional hypothesis for the normal stress leads to a relation for the effective bending stiffness that incorrectly takes into account the presence of residual surface stresses. In particular, studying the phenomenon of self-buckling of a rectangular nanoplate made of different materials, such as Ni[111] and Si[100] with different surface crystallographic direction and negative residual surface stresses, it was revealed that models relying on hypotheses on the normal stress component lead to overestimated values for the critical dimensions of a nanoplate.

This paper pursues two goals. Firstly, we will reconsider the problem of pull-in instability of a nanocantilever based on the novel model presented by Mikhasev (2025) and Mikhasev and Le (2024) free of any hypotheses, and we will focus on the case where residual surface stresses take place on the beam surfaces. Secondly, we propose a novel approach based on replacing the original differential equation with an equivalent integral equation, as well as approximating the resultant lateral force by a power function of the axial coordinate with unknown power-law exponent, which is found from a matching procedure.

The paper is organized as follows. In Section 2, we introduce the physical and mathematical models of a nanocantilever subject to the electrostatic and intermolecular forces. In Section 3, the Bernoulli–Euler type equation with corresponding boundary conditions is reduced to an equivalent non-linear integral equation. Approximating the resultant lateral force by an arbitrary power-law function of the axial coordinate, in Section 4, we give two solutions of the integral equations depending on the sign of residual surface stress. Resolving the extremum problem for the electric voltage as an implicit function of the tip deflection, the pull-in voltage is determined in Section 5. The effects of the dimensionless (normalized) residual surface stress on the pull-in voltage and tip deflection are also

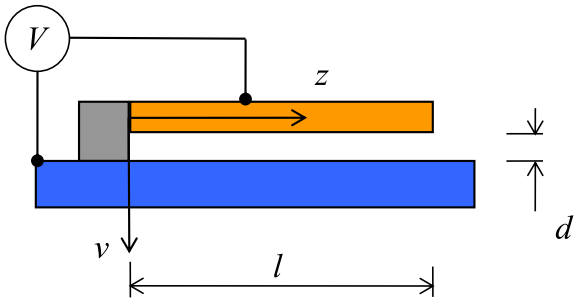

Fig. 1. A micro/nanocantilever beam under electrostatic loading.

analyzed here for different values of the fringing field parameter and the beam aspect ratio. As an example, the pull-in instability of the nanocantilever made of Silicon with crystallographic direction [100] on faces is considered in Section 6. Finally, in Section 7, we draw some conclusions about the residual surface stress effect on the pull-in voltage.

2. Physical and mathematical models

Consider a nanocantilever of length l, width b and thickness h suspended under a fixed electrode, as shown in Fig. 1. The cantilever and fixed electrode are separated by a dielectric spacer with an initial gap d. The beam material is elastic and isotropic with the Young modulus E and Poisson's ratio ν. Assuming that the beam thickness varies at the nanoscale, we take into account the surface effects in the framework of the Gurtin-Murdoch surface elasticity theory (Gurtin & Murdoch, 1975, 1978). Let $E_s^{\pm}$ be the surface moduli of elasticity, and $\tau_0^{\pm}$ the residual surface stresses, where the signs − and + denote quantities placed on the lower and upper surfaces of the beam, respectively.

With reference to Fig. 1, the deflection $v(z)$ of the nanocantilever, where $0 \le z \le l$, clamped at $z = 0$ and subject to electrostatic actuation with the effects of fringing field, and to the effects of intermolecular surface forces and surface elastic stresses, is described by the following non-linear ordinary differential equation (ODE) written in terms of dimensionless variables $u = v/d$, $x = z/l$ (Mikhasev & Le, 2024):

$$\frac{d^4u}{dx^4} - T_0\frac{d^2u}{dx^2} = F(u(x)), \tag{1}$$

where

$$T_0 = \frac{2bl^2\tau_0}{(EI)_{eff}}, \quad (EI)_{eff} = bh^2\left(\frac{hE}{12} + \frac{E_s}{2} + \frac{2\tau_0}{5}\right). \tag{2}$$

Here b is the width of beam cross section, $\tau_0 = \tau_0^+ + \tau_0^-$ is the effective residual surface stress, $E_s = E_s^+ + E_s^-$ is the effective surface Young modulus, $(EI)_{eff}$ is the effective bending rigidity of the beam incorporating both the surface elasticity effect and the residual surface stresses as well, E is Young's modulus of the beam material, $\varepsilon = h/l$ is the beam aspect ratio, and $F(u)$ is the effective dimensionless lateral force, which within the framework of the Timoshenko–Reissner type model (Mikhasev, 2025; Mikhasev & Le, 2024) is defined as

$$F(u) = f(u) - \frac{1}{5}\varepsilon^2\frac{\partial^2 f(u)}{\partial x^2}, \tag{3}$$

with

$$f(u) = \frac{\gamma\beta}{1-u} + \frac{\beta}{(1-u)^2} + \frac{\alpha_W}{(1-u)^3} + \frac{\alpha_C}{(1-u)^4}, \tag{4}$$

being $\gamma = 0.65d/b$ the fringing coefficient and β, α_W and α_C are non-dimensional positive parameters proportional to the electrostatic, van der Waals and Casimir forces, respectively, namely

$$\beta = \frac{\varepsilon_0 bV^2l^4}{2d^3(EI)_{eff}}, \quad \alpha_W = \frac{Abl^4}{6\pi d^4(EI)_{eff}}, \quad \alpha_C = \frac{\pi^2\hbar cbl^4}{240d^5(EI)_{eff}}. \tag{5}$$

In Eqs. (5), $\varepsilon_0 = 8.854\cdot 10^{-12}$ $\mathrm{C^2N^{-1}m^{-2}}$ is the permittivity of vacuum, $\hbar = 1.055\cdot 10^{-34}$ Js is the Planck's constant divided by 2π, $c = 2.998\cdot 10^8$ m/s is the speed of light, A is Hamaker constant, V is the electric voltage applied to the electrodes.

The boundary conditions for a cantilever beam must be imposed at both ends, namely

$$u(0) = 0, \quad u'(0) = 0, \quad u''(1) = 0, \quad u'''(1) - T_0u'(1) = 0. \tag{6}$$

We note that in contrast to the traditional hypotheses-based models (e.g. see Ansari et al., 2014; Ansaria et al., 2014; Farrokhabadi et al., 2016), the effective bending stiffness $(EI)_{eff}$ calculated by Eq. (2) contains the term proportional to the effective residual

surface stress τ_0. Depending on the beam material and the surface crystallographic direction, the parameter τ_0 can be negative or positive, the case $\tau_0 > 0$ corresponding to the tensile effective residual stress, and the inequality $\tau_0 < 0$ relating to the compressive one. In general, the effective bending stiffness $(EI)_{eff}$ is positive. The case $(EI)_{eff} = 0$ can take place only theoretically for ultra-thin beam if $E_s < 0$ and $\tau_0 < 0$, and corresponds to the phenomenon of self-instability (Mikhasev, 2025).

3. Equivalent integral equations

Let us consider first the case of not negative residual surface stress τ_0, which results in the inequality $k^2 = T_0 \geq 0$. The boundary value problem defined by Eqs. (1) and (6) for this case can be replaced by the following equivalent nonlinear integral equation

$$\begin{aligned} u(x) = {} & \frac{1}{k^3}\int_0^x \{kt - \sinh kt + (\cosh kt - 1)\,[\sinh kx - (\cosh kx - 1)\tanh k]\}\, F(u(t))dt \\ & + \frac{1}{k^3}\int_x^1 \{kx - \sinh kx + (\cosh kx - 1)\,[\sinh kt - (\cosh kt - 1)\tanh k]\}\, F(u(t))dt, \end{aligned} \tag{7}$$

which was derived by Radi et al. (2021) using the Green's function for the cantilever Euler–Bernoulli (EB) beam.

Note that both the governing differential Eq. (1) and the integral equation Eq. (7) recover the corresponding formulation for a classical EB cantilever beam as the parameter k tends to 0.

If $\tau_0 < 0$, then the integral equation equivalent to the boundary value problem Eqs. (1), (6) reads (Radi, Bianchi, & di Ruvo, 2017)

$$\begin{aligned} u(x) = {} & \frac{1}{k^3}\int_0^x \{\sin kt - kt + (1 - \cos kt)\,[\sin kx + (1 - \cos kx)\tan k]\}\, F(u(t))dt \\ & + \frac{1}{k^3}\int_x^1 \{\sin kx - kx + (1 - \cos kx)\,[\sin kt + (1 - \cos kt)\tan k]\}\, F(u(t))dt, \end{aligned} \tag{8}$$

which is obtained form Eq. (7) by replacing k with ik, where $i^2 = -1$ and $k^2 = -T_0 > 0$.

Note that in the case $T_0 < 0$, Eq. (1) is similar to the governing equation for a cantilever nanobeam of length l and bending rigidity EI compressed by an axial load $P = T_0 EI/l^2$, whose buckling load occurs for $k = \pi/2$.

4. Simplified model based on the approximation of the load distribution

Due to the nonlinearity of the electrostatic force acting on the cantilever, the boundary value problem defined by Eqs. (1), (6) as well as the equivalent integral Eqs. (7), (8) do not allow an exact solution in the explicit form. Here, we use an approach based on the approximation of the load distribution by an arbitrary power-law function of the nondimensional abscissa s, namely

$$f_n(s) = f(0) + [f(u_T) - f(0)]s^n, \tag{9}$$

for $0 \leq s \leq 1$, where $u_T = u(1)$ denotes the unknown tip deflection and $n > 1$ is an unknown real parameter to be determined by matching procedure illustrated in the following and

$$\begin{aligned} & f(0) = \gamma\beta + \beta + \alpha_W + \alpha_C, \\ & f(u_T) = \frac{\gamma\beta}{1 - u_T} + \frac{\beta}{(1 - u_T)^2} + \frac{\alpha_W}{(1 - u_T)^3} + \frac{\alpha_C}{(1 - u_T)^4}. \end{aligned} \tag{10}$$

Note that $f_n(0) = f(0)$ and $f_n(1) = f(u_T)$, namely the approximated loading function (9) always coincides with the actual loading function (4) at $s = 0$ and $s = 1$. Correspondingly, the right-hand member (3) of the governing Eq. (1) can be approximated by

$$F_n(s) = f(0) + [f(u_T) - f(0)]\left[s^n - \varepsilon^2 n(n-1)s^{n-2}/5\right]. \tag{11}$$

Instead of assuming a specific deflection shape in terms of some unknown parameters, which could be determined by using the Rayleigh–Ritz method, here we choose to approximate the loading distribution $f(u)$ by considering the shape function (9) which varies with the magnitude of the applied loading, since the power-law exponent n varies with load magnitude β as well as the tip displacement u_T.

Note that the linear distributed load (LDL) model with $n = 1$ and $f_0 = f(0) = 0$ was considered in Yang et al. (2008) in the framework of the stress gradient theory of nonlocal elasticity, while LDL model and the quadratic distributed load (QDL) model with $n = 2$ and $f(0) = \gamma\beta + \beta + \alpha_W + \alpha_C$ were elaborated in our contributions (Mikhasev, Radi, & Misnik, 2022, 2024) in the framework of the nonlocal theory of elasticity.

4.1. Case of not negative residual surface stress

Consider the case when $\tau_0 \geq 0$. Then according to Eq. (7) the beam deflection produced by the approximated load distribution (9) is given by

$$\begin{aligned} u_n(x) = {} & \frac{1}{k^3}\int_0^x \{kt - \sinh kt + (\cosh kt - 1)\,[\sinh kx - (\cosh kx - 1)\tanh k]\}\, F_n(t)dt \\ & + \frac{1}{k^3}\int_x^1 \{kx - \sinh kx + (\cosh kx - 1)\,[\sinh kt - (\cosh kt - 1)\tanh k]\}\, F_n(t)dt. \end{aligned} \tag{12}$$

In particular, for $x = 1/2$ and $x = 1$, from (12) one has

$$u_n(x) = \frac{1}{k^3}\int_0^{1/2}\left\{kt - \sinh kt + (\cosh kt - 1)\left[\sinh\frac{k}{2} - \left(\cosh\frac{k}{2} - 1\right)\tanh k\right]\right\}F_n(t)dt + \frac{1}{k^3}\int_{1/2}^{1}\left\{\frac{k}{2} - \sinh\frac{k}{2} + \left(\cosh\frac{k}{2} - 1\right)[\sinh kt - (\cosh kt - 1)\tanh k]\right\}F_n(t)dt, \tag{13}$$

and

$$u_n(1) = \frac{1}{k^3}\int_0^1 [kt - \sinh kt + (\cosh kt - 1)\tanh k]F_n(t)dt, \tag{14}$$

respectively. By using Eq. (9) and the definite integrals (A.1)–(A.4) provided in Appendix A, Eqs. (13) and (14) can be evaluated as

$$\begin{aligned} u_n(1/2) = {} & \frac{f(0)}{k^4}\left[\frac{3k^2}{8} + \frac{1}{\cosh k}\left(\cosh\frac{k}{2} - 1 + k\sinh\frac{k}{2} - k\sinh k\right)\right] + \frac{f(u_T) - f(0)}{k^3}\left\{\frac{k}{1+n}\left(\frac{1}{2} - \frac{2^{-2-n}}{2+n}\right)\right. \\ & + \left(\cosh\frac{k}{2} - 1\right)\left[\mathrm{Sh}\left(n,\frac{1}{2},1\right) - \mathrm{Ch}\left(n,\frac{1}{2},1\right)\tanh k\right] + \frac{\sinh(k/2) - \sinh k}{\cosh k}\left[\frac{1}{1+n} - \mathrm{Ch}\left(n,0,\frac{1}{2}\right)\right] - \mathrm{Sh}\left(n,0,\frac{1}{2}\right) \\ & - \frac{\varepsilon^2}{5}n(n-1)\left[\frac{k}{n-1}\left(\frac{1}{2} - \frac{1}{2^n n}\right) + \left(\cosh\frac{k}{2} - 1\right)\left(\mathrm{Sh}\left(n-2,\frac{1}{2},1\right) - \mathrm{Ch}\left(n-2,\frac{1}{2},1\right)\tanh k\right)\right. \\ & \left.\left. + \frac{\sinh(k/2) - \sinh k}{\cosh k}\left(\frac{1}{n-1} - \mathrm{Ch}\left(n-2,0,\frac{1}{2}\right)\right) - \mathrm{Sh}\left(n-2,0,\frac{1}{2}\right)\right]\right\}, \end{aligned} \tag{15}$$

$$\begin{aligned} u_n(1) = {} & \frac{f(0)}{k^4}\left(1 + \frac{k^2}{2} - \frac{1}{\cosh k} - k\tanh k\right) - \frac{f(u_T) - f(0)}{k^3}\left\{\left[\mathrm{Sh}(n,0,1) - \mathrm{Ch}(n,0,1)\tanh k\right] + \frac{\tanh k}{n+1} - \frac{k}{n+2}\right. \\ & \left. - \frac{\varepsilon^2}{5}(n-1)n\left[\frac{\tanh k}{n-1} - \frac{k}{n} + (\mathrm{Sh}(n-2,0,1) - \mathrm{Ch}(n-2,0,1)\tanh k)\right]\right\}, \end{aligned} \tag{16}$$

where

$$\begin{aligned} \mathrm{Sh}(n,a,b) &= \int_a^b t^n \sinh kt dt = 2^{-1}k^{-1-n}\left\{\mathrm{e}^{-\mathrm{i}n\pi}\left[\Gamma(1+n,-bk) - \Gamma(1+n,-ak)\right] + \Gamma(1+n,bk) - \Gamma(1+n,ak)\right\}, \\ \mathrm{Ch}(n,a,b) &= \int_a^b t^n \cosh kt dt = 2^{-1}k^{-1-n}\left\{\mathrm{e}^{-\mathrm{i}n\pi}\left[\Gamma(1+n,-bk) - \Gamma(1+n,-ak)\right] - \Gamma(1+n,bk) + \Gamma(1+n,ak)\right\}, \end{aligned} \tag{17}$$

are real-valued functions for $n > 0$ and $k > 0$, being $\Gamma(a,b)$ the incomplete gamma function and $\Gamma(a,0) = \Gamma(a)$ the gamma function.

4.2. Case of negative residual surface stress

Now, let $\tau_0 < 0$. Then the beam deflection under the lateral force approximated by function (9) will be evaluated by Eq. (8), where $F(u(t))$ is to be replaced with $F_n(t)$. Then for $x = 1/2$ and $x = 1$ one has

$$\begin{aligned} u_n(1/2) = {} & \frac{f(0)}{k^4\cos k}\left(1 - \cos\frac{k}{2} + \frac{3k^2}{8}\cos k + k\sin\frac{k}{2} - k\sin k\right) + \frac{f(u_T) - f(0)}{k^3}\left\{-\frac{\left(n+2-2^{-n-1}\right)k}{2(n+1)(n+2)}\right. \\ & + \frac{\sin k - \sin(k/2)}{\cos k}\left[\frac{1}{n+1} - \mathrm{C}\left(n,0,\frac{1}{2}\right)\right] + \mathrm{S}\left(n,0,\frac{1}{2}\right) + \left(1 - \cos\frac{k}{2}\right)\left[\mathrm{S}\left(n,\frac{1}{2},1\right) - \mathrm{C}\left(n,\frac{1}{2},1\right)\tan k\right] \\ & - \frac{\varepsilon^2}{5}n(n-1)\left[-\frac{\left(n-2^{1-n}\right)k}{2n(n-1)} + \frac{\sin k - \sin(k/2)}{\cos k}\left(\frac{1}{n-1} - \mathrm{C}\left(n-2,0,\frac{1}{2}\right)\right) + \mathrm{S}\left(n-2,0,\frac{1}{2}\right)\right. \\ & \left.\left. + \left(1 - \cos\frac{k}{2}\right)\left(\mathrm{S}\left(n-2,\frac{1}{2},1\right) - \mathrm{C}\left(n-2,\frac{1}{2},1\right)\tan k\right)\right]\right\}, \end{aligned} \tag{18}$$

$$\begin{aligned} u_n(1) = {} & \frac{f(0)}{k^4}\left(1 - \frac{1}{\cos k} - \frac{k^2}{2} + k\tan k\right) + \frac{f(u_T) - f(0)}{k^3}\left\{\frac{\tan k}{n+1} - \frac{k}{n+2} + \mathrm{S}(n,0,1) - \mathrm{C}(n,0,1)\tan k\right. \\ & \left. - \frac{\varepsilon^2}{5}n(n-1)\left[\frac{\tan k}{n-1} - \frac{k}{n} + \mathrm{S}(n-2,0,1) - \mathrm{C}(n-2,0,1)\tan k\right]\right\}, \end{aligned} \tag{19}$$

where

$$\begin{aligned} \mathrm{S}(n,a,b) &= \int_a^b t^n \sin kt dt = \frac{1}{k^{n+1}}\mathrm{Re}\left\{\mathrm{e}^{-\mathrm{i}n\pi/2}[\Gamma(n+1,\mathrm{i}ak) - \Gamma(n+1,\mathrm{i}bk)]\right\}, \\ \mathrm{C}(n,a,b) &= \int_a^b t^n \cos kt dt = \frac{1}{k^{n+1}}\mathrm{Im}\left\{\mathrm{e}^{-\mathrm{i}n\pi/2}[\Gamma(n+1,\mathrm{i}ak) - \Gamma(n+1,\mathrm{i}bk)]\right\}. \end{aligned} \tag{20}$$

5. Estimation of pull-in voltage

Let us impose the approximated conditions

$$u_T(1) = u_T, \quad f_n(1/2) = f(u_n(1/2)). \tag{21}$$

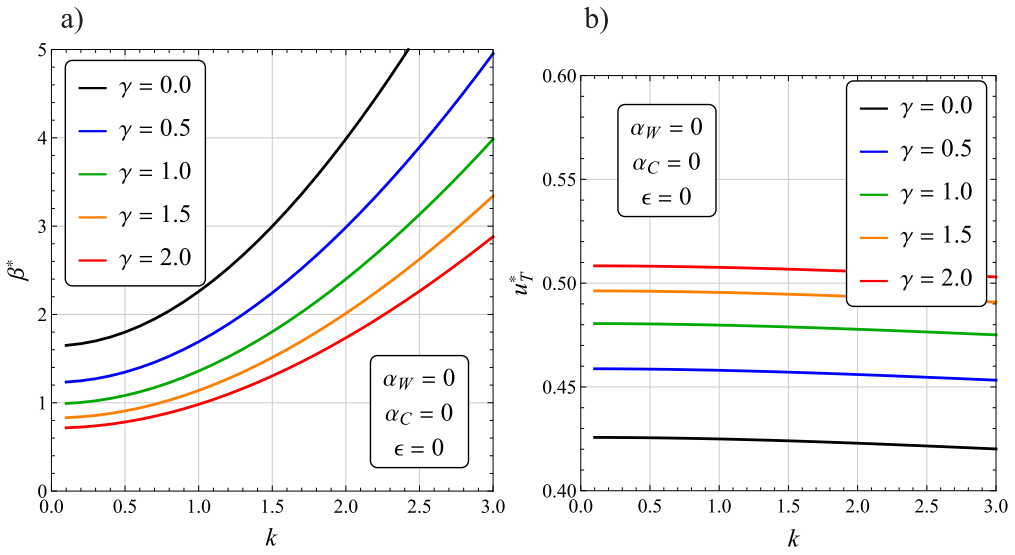

Fig. 2. Variation of the pull-in electrostatic load β^* (a) and tip deflection u_T^* (b) with the surface elasticity parameter k for some values of the fringing field parameter γ, in the absence of intermolecular forces.

The latter condition requires that the approximate load distribution of the lateral force (8) calculated at $x = 1/2$ must coincide with the load calculated from Eq. (4), where the deflection is obtained from Eq. (15) or Eq. (8) depending on the sign of the residual surface stress τ_0. The pair of Eqs. (21) with relations (9), (15), (16) or (9), (18), (19) for the cases $\tau_0 \geq 0$ and $\tau_0 < 0$, respectively, define a system of two nonlinear algebraic equations for the unknown parameters u_T and n as functions of the loading parameters β, α_W and α_C. The maximum attained by the implicit function $\beta(u_T)$ then provides the approximated values of the pull-in voltage β^* and deflection u_T^*.

5.1. Critical parameters in the case of positive residual stress

At first, let us consider the case $\tau_0 \geq 0$. A numerical maximization of the implicit function $\beta(u_T)$ for some values of the fringing field parameter γ in the absence of intermolecular forces ($\alpha_W = \alpha_C = 0$), ignoring the correcting term in Eq. (3) (namely for $\varepsilon = 0$), yields the results reported in Figs. 2. It is clearly seen that increasing the positive (stretching) residual surface stress τ_0 results in increasing the pull-in electrostatic voltage β^* and decreasing the corresponding critical tip deflection u_T^* for any value of γ. As for the effect of the parameter γ, its increase at a fixed value of k, as expected, leads to a decrease in β^* and an increase in u_T^*, respectively. Fig. 3 displays a quite new result about the variation of the power-law exponent n^* under the pull-in electrostatic load with the surface elasticity parameter $k \geq 0$ for $\alpha_W = \alpha_C = 0, \varepsilon = 0$ and some values of the fringing parameter γ. The lateral force (9) indeed is neither a linear or quadratic function of the axial coordinate x, as was assumed in contributions (Mikhasev et al., 2022; Yang et al., 2008), but it displays a higher power-law exponent $n^* > 2$ for small and positive values of the residual surface stress. However, increasing the parameter k, the power-law exponent n^* decreases and reaches the value $n^* = 2$ at $k \approx 2.6$ if $\gamma = 0$, and at larger values of k if the fringing parameter γ is accounted.

Similar calculations were performed for fixed $\alpha_W = \alpha_C = \gamma = 0$ and different values of the small parameter ε, which was introduced in Mikhasev and Le (2024) and Mikhasev (2025) within the framework of the Timoshenko–Reissner model for shear-deformable beams and plates. Figs. 4 and 5 demonstrate that the effect of the beam aspect ratio ε on the dimensionless pull-in voltage β^*, tip deflection u_T^* and power-law exponent n^* is small: the values of β^*, u_T^* and n^* slightly increasing together with the parameter ε for any fixed value of k.

5.2. Critical parameters in the case of negative residual stress

Consider the scenario when the residual surface stress is negative ($\tau_0 < 0$). To remind, here $T_0 < 0$, $k^2 = -T_0$ and all calculations are performed using Eqs. (18), (19) and (21). In this case, a numerical maximization of the implicit function $\beta(u_T)$ results in the approximated values of the pull-in voltage β^* and the critical tip deflection u_T^* provided in Fig. 6.

As expected for $\tau_0 < 0$, the pull-in voltage decreases as the parameter k increases and it tends to 0 as k approaches $\pi/2$, which corresponds to the buckling load for the cantilever beam. Again, the increase of the beam aspect ratio ε yields a small increment of the pull-in voltage and pull-in tip deflection. In contrast to the case of $\tau_0 \geq 0$, Fig. 7 shows that increasing the surface elasticity parameter k for $\tau_0 < 0$ results in increasing the power-law exponent n^*.

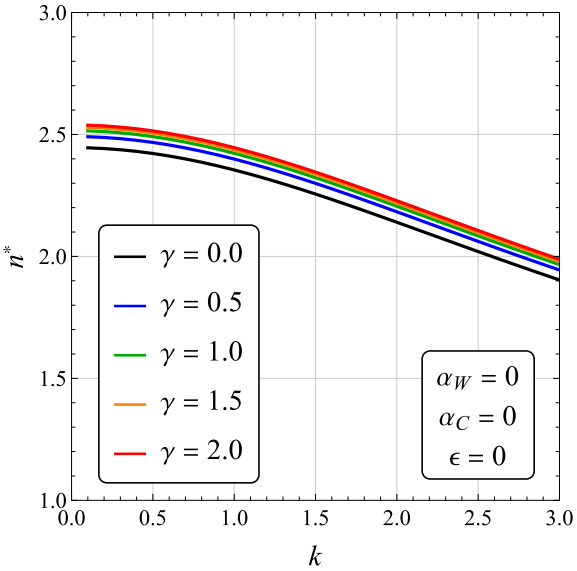

Fig. 3. Variation of the power-law exponent n^* under the pull-in electrostatic load with the surface elasticity parameter k for some values of the fringing field parameter γ, in the absence of intermolecular forces.

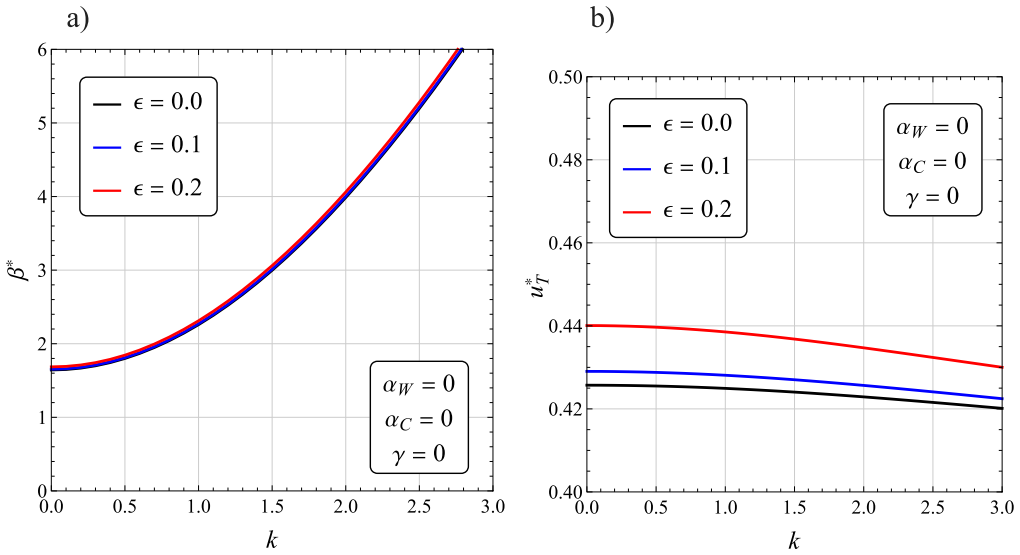

Fig. 4. Variation of the pull-in electrostatic load β^* (a) and tip deflection u_T^* (b) with the surface elasticity parameter k for five different values of the aspect ratio ϵ, in the absence of intermolecular forces.

6. Example

Let us consider a nanocantilever made of Silicon with the crystallographic direction [100] on surfaces. The input parameters for such nanobeam are the following (Miller & Shenoy, 2000; Shenoy, 2005):

$$E = 130 \text{ GPa}, \quad \nu = 0.24, \quad E_s = -11.5 \text{ N/m}, \quad \tau_0 = -0.505 \text{ N/m}.$$

The surface elastic modulus was calculated as

$$E_s = \frac{\left(S_{1111} + 2S_{1122}\right)\left(S_{1111} - S_{1122}\right)}{S_{1111} + S_{1122}}, \tag{22}$$

where S_{ijkl} are components of the 4th order rank surface elasticity tensor defined by the atomistic simulation (Shenoy, 2005).

Figs. 8 and 9 display the variation of the pull-in voltage V^*, normalized pull-in tip deflection u_T^*, and power-law exponent n^* under the pull-in voltage with the beam length l, for different heights of the nanobeam cross section $h = 5, 8, 10$ nm (curves 1, 2,

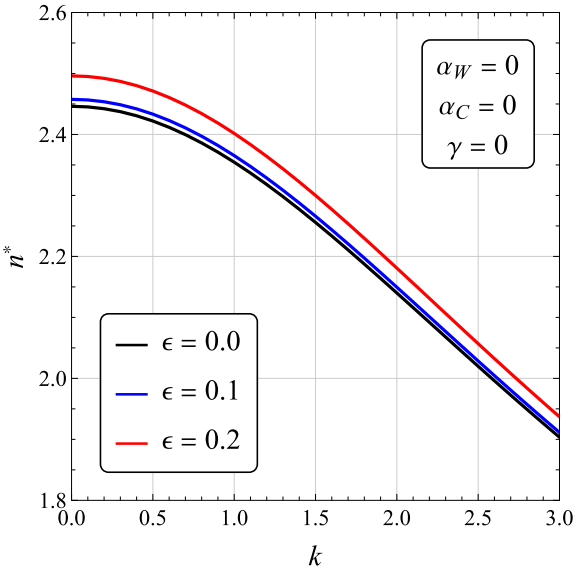

Fig. 5. Variation of the power-law exponent n^* under the pull-in electrostatic load with the surface elasticity parameter k for five different values of the aspect ratio ϵ, in the absence of intermolecular forces.

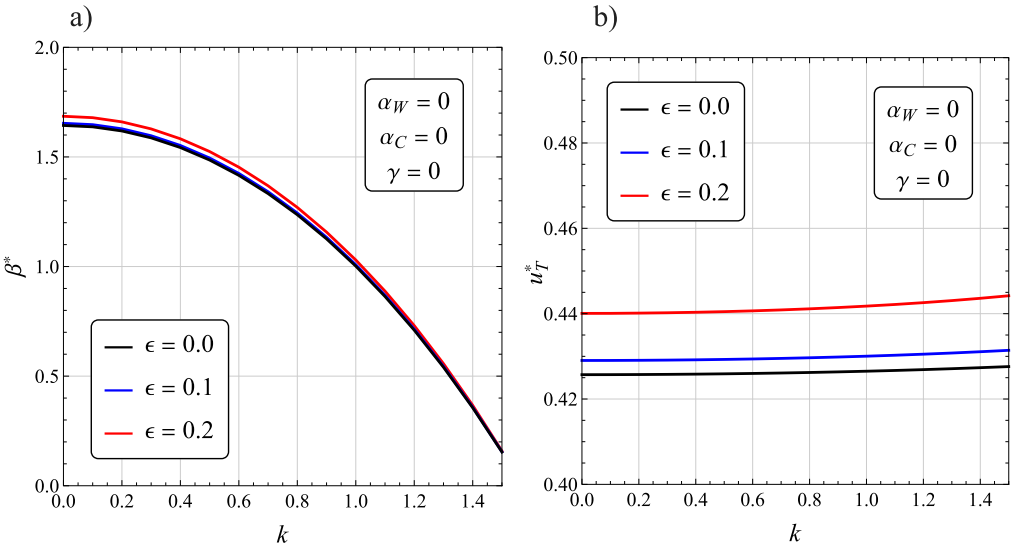

Fig. 6. Variation of the pull-in electrostatic load β^* (a) and tip deflection u_T^* (b) with the surface elasticity parameter k for $\tau_0 < 0$, and for five different values of the aspect ratio ϵ, in the absence of intermolecular attraction for $\gamma = 0$.

3, respectively). The solid lines were plotted taking into account the negative (compressive) residual stresses τ_0, while dashed ones correspond to the cases when the residual stresses are ignored ($\tau_0 = 0$). The effects of intermolecular forces and fringing field are ignored in these figures, which thus hold for $d \ll b$. The analysis of these plots shows that the presence of a negative residual surface stress can significantly affect the critical values of electrostatic voltage and tip deflection as well as the power-law exponent. The negative stress τ_0 reduces the pull-in voltage and increases the corresponding tip deflection. This effect becoming more pronounced if the beam height h is decreased, thus resulting in the so-called phenomenon of self-buckling (Mikhasev, 2025) without an applied electrostatic voltage at some critical values of parameters h and l, which satisfy the condition $k = \pi/2$, namely

$$l = \frac{\pi}{4} h \sqrt{-\frac{Eh}{6\tau_0} - \frac{E_s}{\tau_0} - \frac{4}{5}}. \tag{23}$$

We note that the self-instability of nanoplates made of different materials due to a negative residual surface stress was in detail studied in Mikhasev (2025). In particular, it was shown that this effect can occur for ultrathin square plates made of Silicon and

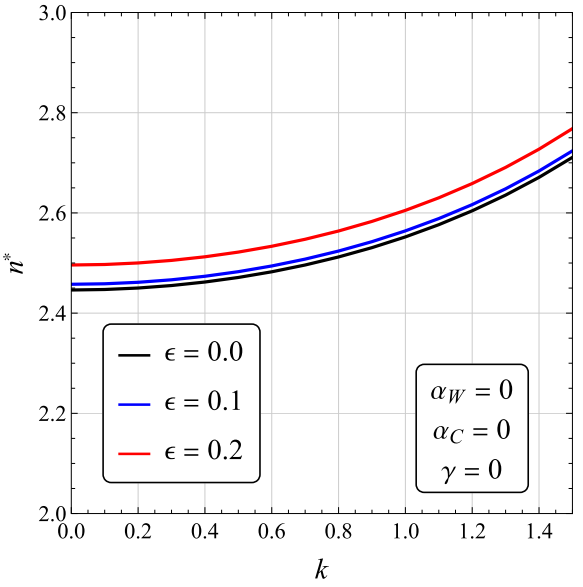

Fig. 7. Variation of the power-law exponent n^* under the pull-in electrostatic load with the surface elasticity parameter k for $\tau_0 < 0$, and for five different values of the aspect ratio ϵ, in the absence of intermolecular attraction for $\gamma = 0$.

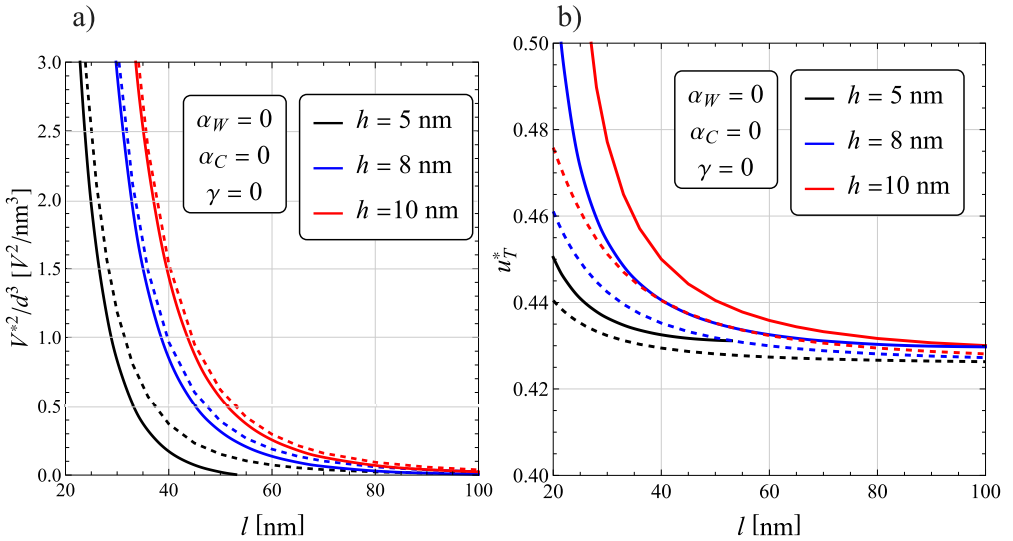

Fig. 8. Variation of the ratio V^{*2}/d^3 (a) and the tip deflection u_T^* (b) with the span l of the Si[100] nanocantilever, for three different heights of the beam cross section h, in the absence of intermolecular attraction for $\gamma = 0$. The dashed curves correspond to the cases when the residual stresses are ignored ($\tau_0 = 0$).

Nickel with the surface crystallographic directions [100] and [111], respectively, if their geometric dimensions reach some critical values. The effect of a negative stress τ_0 on the power-law exponent n^* turns out to be more complex and depends on the beam length l and height h. As seen, for every height h there exists a nanobeam length $l = l_m$ for which the function $n^*(l)$ attains a local minimum, so that for $l > l_m$, the power-law exponent $n^*(l)$ is an increasing function of the beam length l, while for a beam without residual surface stresses $n^*(l)$ is a monotonically decreasing function.

As explained in Lamoreaux (2005) and considered in Radi et al. (2017), the effects of van der Waals interaction are significant for small distance gap between the electrodes, namely for $d < 20$ nm, whereas for $d > 20$ nm the Casimir interaction become prevalent. These effects are contemplated in Fig. 10, where the variations of the pull-in voltage V^* with the length l of the Si [100] nanocantilever are plotted for three different gap distance d, neglecting the effect of the fringing field, namely for $d \ll b$. Three different gap distances between the electrodes are considered in the examples, namely $d = 5, 10$, and 15 nm, thus involving van der Waals interactions. The Hamaker constant occurring in Eq. $(2)_2$ is taken as $A = 2.96 \times 10^{-19}$ J. It corresponds to the interaction between Silicon and highly oriented Pyrolytic Graphite (Lee, Howell, Raman, & Reifenberger, 2003). According to the height h of

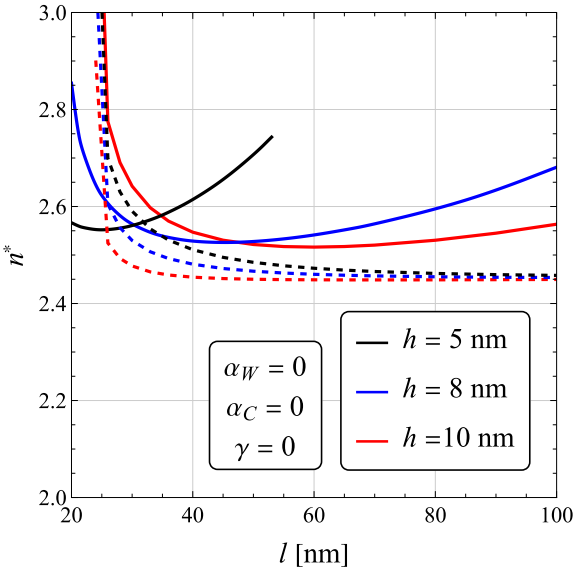

Fig. 9. Variation of the power-law exponent n^* under the pull-in voltage with the length l of the Si[100] nanocantilever, for three different heights of the beam cross section$h$, in the absence of intermolecular attraction for $\gamma = 0$. The dashed curves correspond to the cases when the residual stresses are ignored ($\tau_0 = 0$).

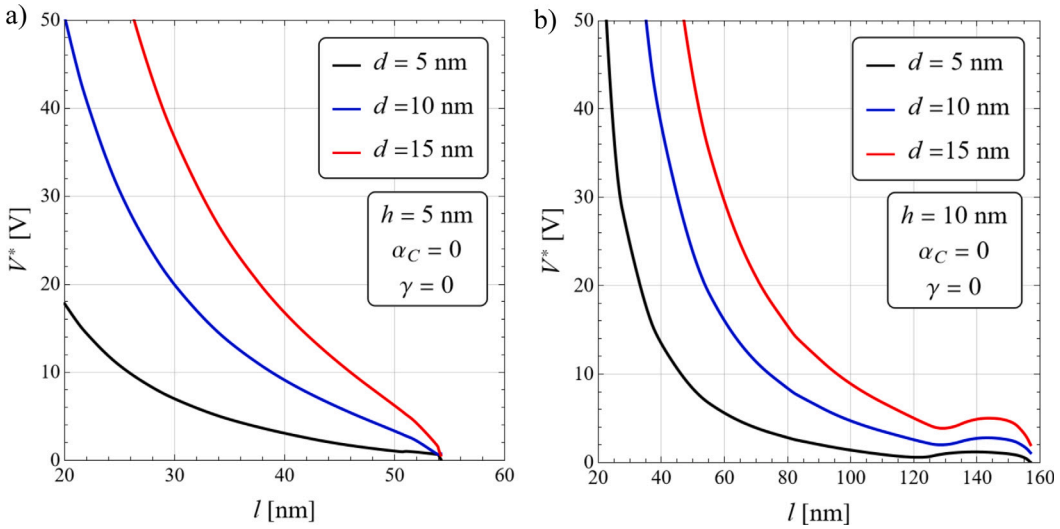

Fig. 10. Variation of the pull-in voltage V^* with the length l of the Si[100] nanocantilever, for three different gap distance d, both for a) $h = 5$ nm and b) $h = 10$ nm, in the presence of van der Waals interaction for $\gamma = 0$.

the cross section, there exist a limit value l_b of the cantilever length which causes buckling instability (self-buckling) due to the effect of compressive residual surface stress only, occurring for $k = \pi/2$. According to Eq. (23), the limit length for the Silicon [100] nanocantilever of height $h = 5$ nm is $l_b = 54.1$ nm, whereas for $h = 10$ nm is $l_b = 158.1$ nm. Figs. 10 shows that the pull-in voltage rapidly decays as the nanocantilever length increases and tends to its limit buckling length. Moreover, it also decreases for a small distance gap between the electrodes.

7. Approximate expression for the pull-in voltage

On the basis of the results provided by the present analysis, the following approximate expressions for a ready calculation of the normalized pull-in voltage can be derived. It accounts for the surface effects including the residual surface stresses, but it neglects the effects of intermolecular forces:

$$\tilde{\beta} = 1.65\left(1+\frac{\epsilon^2}{2}\right)\frac{\left(1 \pm 4k^2/\pi^2\right)^{0.9}}{(1+\gamma)^{0.8}}, \tag{24}$$

where the upper (lower) sign holds for $\tau_0 > 0$ ($\tau_0 < 0$). Eq. (24) provides an acceptable approximation of β^* for $\tau_0 < 0$, as well as for $\tau_0 > 0$ and $k < 5$. The corresponding approximate pull-in voltage is then given by the relation

$$\tilde{V} = \frac{dh}{l^2(1+\gamma)^{0.4}}\left[1 \mp \frac{480l^2\tau_0}{\pi^2h^2\left(5Eh+30E_s+24\tau_0\right)}\right]^{0.45}\sqrt{\frac{3.3d}{\epsilon_0}\left(\frac{Eh}{12}+\frac{E_s}{2}+\frac{2\tau_0}{5}\right)\left(1+\frac{h^2}{2l^2}\right)}. \tag{25}$$

A comparison between the results obtained by using the approximate expression (24) for the normalized pull-in voltage, plotted in Figs. S1, S2, and S3 in the Supplementary material, and those reported in Figs. 2a, 4a and 6a, respectively, then validates Eq. (24). Similarly, a comparison between the variations of the pull-in voltage with the Si[100] nanocantilever length l obtained by using the approximate expression (25) plotted in Fig. S4a,b and those reported in Fig. 10a,b, then validates Eq. (25).

8. Conclusions

Using the modified differential equation (Mikhasev & Le, 2024) for the Euler–Bernoulli beam with the effective bending stiffness depending on the surface elastic modulus and residual stresses (Mikhasev, 2025), we reconsidered the problem of the pull-in instability of electrically actuated nanocantilever, taking into account the intermolecular attraction and surface stresses. Depending on the sign of residual surface stresses, the original differential equation with corresponding boundary conditions was reduced to an equivalent nonlinear integral equation. We proposed a novel approach based on the approximation of the resultant lateral force by an arbitrary power-law function of the axial coordinate, which allowed us to solve the integral equations explicitly. The solutions to the integral equations were then used to derive transcendental algebraic equations for the electric voltage as an implicit function of the tip deflection. Considering the extremum problem for these implicit functions, we plotted the pull-in voltage versus the normalized residual surface stress at different values of geometric and constitutive parameters. First, we observed that the power-law exponent in the polynomial approximating the resultant lateral force is not equal to 1 or 2, as it was assumed in previous contributions (Mikhasev et al., 2022, 2024; Yang et al., 2008), but it varies in the wide range, approximately from 1 to 3, together with the magnitude of residual surface stress, and depend on all input parameters, including the aspect ratio. Then, the analysis of plots revealed that a positive residual surface stress yields a growth of the pull-in voltage, thus coinciding with the conclusion drown in Ansari et al. (2014), Farrokhabadi et al. (2016) and Radi et al. (2021), while the presence of negative residual stress leads to decreasing the pull-in voltage, which can be dramatic depending on the beam height and length. Considering, as an example, the nanocantilever made of Silicon [100], we discovered a novel effect: for a very thin nanobeam, there exists a critical length for which the nanocantilever turns out to be unstable. This phenomenon, called as self-buckling due to negative (compressive) surface residual stresses (Mikhasev, 2025), does not depend on the gap between the cantilever and the fixed electrode, it precedes the pull-in instability and occurs at zero electric voltage. Moreover, an approximate expression for a ready calculation of the pull-in voltage has been proposed.

The results presented here can be relevant for the accurate design of micro and nano-switches containing a cantilever beam as a sensitive element, that corresponds to the current trend of minimizing the size of devices as much as possible. Finally note, the approach developed in the paper can be also extended for studying pull-in instability of electrically actuated thin circular plates.

CRediT authorship contribution statement

Gennadi I. Mikhasev: Writing – review & editing, Investigation, Formal analysis, Conceptualization. **Enrico Radi:** Writing – review & editing, Writing – original draft, Software, Methodology, Investigation, Formal analysis.

Declaration of competing interest

The authors declare that they have no known competing financial interests or personal relationships that could have appeared to influence the work reported in this paper.

Acknowledgments

G.I.M. acknowledges the support from the Harbin Institute of Technology, China, within the framework of the start-up research grant. E.R. is grateful to the Italian “Gruppo Nazionale di Fisica Matematica” INdAM-GNFM for support.

Appendix A

The following definite integral are used in the calculation of Eqs. (13), (14):

$$\int_0^{1/2} t^n \sinh ktdt = \frac{1}{2}\int_0^{1/2} t^n\left(e^{kt}-e^{-kt}\right)dt = \frac{e^{-i\pi n}\left[\Gamma(1+n,-k/2)-\Gamma(1+n)\right]+\Gamma(1+n,k/2)-\Gamma(1+n)}{2k^{1+n}}, \tag{A.1}$$

$$\int_0^{1/2} t^n \cosh ktdt = \frac{1}{2}\int_0^{1/2} t^n\left(e^{kt}+e^{-kt}\right)dt = \frac{e^{-i\pi n}\left[\Gamma(1+n,-k/2)-\Gamma(1+n)\right]-\Gamma(1+n,k/2)+\Gamma(1+n)}{2k^{1+n}}, \tag{A.2}$$

$$\int_{1/2}^1 t^n \sinh ktdt = \frac{1}{2}\int_{1/2}^1 t^n\left(e^{kt}-e^{-kt}\right)dt = \frac{e^{-i\pi n}\left[\Gamma(1+n,-k)-\Gamma(1+n,-k/2)\right]-\Gamma(1+n,k/2)+\Gamma(1+n,k)}{2k^{1+n}}, \tag{A.3}$$

$$\int_{1/2}^1 t^n \cosh ktdt = \frac{1}{2}\int_{1/2}^1 t^n\left(e^{kt}+e^{-kt}\right)dt = \frac{e^{-i\pi n}\left[\Gamma(1+n,-k)-\Gamma(1+n,-k/2)\right]+\Gamma(1+n,k/2)-\Gamma(1+n,k)}{2k^{1+n}}. \tag{A.4}$$

Appendix B. Supplementary data

Supplementary material related to this article can be found online at https://doi.org/10.1016/j.ijengsci.2025.104356.

Data availability

No data was used for the research described in the article.

References

Altenbach, H., & Eremeyev, V. A. (2011). On the shell theory on the nanoscale with surface stresses. *International Journal in Engineering Sciences*, *49*(12), 1294–1301.

Altenbach, H., & Eremeyev, V. A. (2017). On the elastic plates and shells with residual surface stresses. *Proceedings of the IUTAM*, *21*, 25–32.

Ansari, R., Mohammadi, V., Faghih Shojaei, M., Gholami, R., & Darabi, M. A. (2014). A geometrically non-linear plate model including surface stress effect for the pull-in instability analysis of rectangular nanoplates under hydrostatic and electrostatic actuations. *International Journal of Non-Linear Mechanics*, *67*, 16–26.

Ansaria, R., Gholami, R., Faghih Shojaei, M., Mohammadia, V., & Sahmania, S. (2014). Surface stress effect on the pull-in instability of circular nanoplates. *Acta Astronautica*, *102*, 140–150.

Cuenot, S., Fretigny, C., Demoustier-Champagne, S., & Nysten, B. (2004). Surface tension effect on the mechanical properties of nanomaterials measured by atomic force microscopy. *Physical Review B*, *69*, Article 165410-165415.

Dequesnes, M., Rotkin, S. V., & Aluru, N. R. (2002). Calculation of pull-in voltages for carbon-nanotube-based nanoelectromechanical switches. *Nanotechnology*, *13*, 120–131.

Duan, J. S., & Rach, R. (2013). A pull-in parameter analysis for the cantilever NEMS actuator model including surface energy, fringing field and Casimir effects. *International Journal of Solids and Structures*, *50*, 3511–3518.

Eremeyev, V. A. (2016). On effective properties of materials at the nano-and microscales considering surface effects. *Acta Mechanica*, *227*(1), 29–42.

Farrokhabadi, A., Mohebshahedin, A., Rach, R., & Duan, J. S. (2016). An improved model for the cantilever NEMS actuator including the surface energy, fringing field and Casimir effects. *Physica E: Low-dimensional Systems and Nanostructures*, *75*, 202–209.

Fu, Y., & Zhang, J. (2011). Size-dependent pull-in phenomena in electrically actuated nanobeams incorporating surface energies. *Applied Mathematical Modelling*, *35*, 941–951.

Gurtin, M. E., & Murdoch, A. I. (1975). A continuum theory of elastic material surfaces. *Archive for Rational Mechanics and Analysis*, *57*(4), 291–323.

Gurtin, M. E., & Murdoch, A. I. (1978). Surface stress in solids. *International Journal of Solids and Structures*, *14*(6), 431–440.

Huang, J. M., Liew, K. M., Wong, C. H., Rajendran, S., Tan, M. J., & Liu, A. Q. (2001). Mechanical design and optimization of capacitive micromachined switch. *Sensors and Actuators A: Physical*, *93*, 273–285.

Khaniki, H. B., Ghayesh, M. H., & Amabili, M. (2021). A review on the statics and dynamics of electrically actuated nano and micro structures. *International Journal of Non-Linear Mechanics*, *129*, Article 103658.

Lamoreaux, S. K. (2005). The Casimir force background, experiments, and applications. *Reports on Progress in Physics*, *68*, 201–236.

Lee, S. I., Howell, S. W., Raman, A., & Reifenberger, R. (2003). Nonlinear dynamic perspectives on dynamic force microscopy. *Ultramicroscopy*, *97*, 185–198.

Ma, J. B., Jiang, L., & Asokanthan, S. F. (2010). Influence of surface effects on the pull-in instability of NEMS electrostatic switches. *Nanotechnology*, *21*, Article 505708.

Mikhasev, G. I. (2025). Asymptotic long-wave model for an elastic isotropic nanoplate with surface effects derived from the 3D theory of elasticity and its comparison with hypotheses-based models. *Continuum Mechanics and Thermodynamics*, *37*(2), http://dx.doi.org/10.1007/s00161-025-01366-z.

Mikhasev, G. I., & Le, N. D. (2024). Asymptotic model of the long-wavelength vibrations of an ultrathin beam strip taking into account surface effects. *Vestnik St. Petersburg University: Mathematics*, *57*(3), 383–391.

Mikhasev, G., Radi, E., & Misnik, V. (2022). Pull-in instability analysis of a nanocantilever based on the two-phase nonlocal theory of elasticity. *Journal of Applied and Computational Mechanics*, *8*(4), 1456–1466.

Mikhasev, G., Radi, E., & Misnik, V. (2024). Modeling pull-in instability of CNT nanotweezers under electrostatic and van der Waals attractions based on the nonlocal theory of elasticity. *International Journal of Engineering Science*, *195*, Article 104012.

Miller, R. E., & Shenoy, V. B. (2000). Size-dependent elastic properties of nanosized structural elements. *Nanotechnology*, *11*, 139–147.

Mousavi, T., Bornassi, S., & Haddadpour, H. (2013). The effect of small scale on the pull-in instability of nano-switches using DQM. *International Journal of Solids and Structures*, *50*, Article 11931202.

Radi, E., Bianchi, G., & di Ruvo, L. (2017). Upper and lower bounds for the pull-in parameters of a micro- or nanocantilever on a flexible support. *International Journal of Non-Linear Mechanics*, *92*, 176–186. http://dx.doi.org/10.1016/j.ijnonlinmec.2017.03.011.

Radi, E., Bianchi, G., & di Ruvo, L. (2018). Analytical bounds for the electromechanical buckling of a compressed nanocantilever. *Applied Mathematical Modelling*, *59*, 571–582.

Radi, E., Bianchi, G., & Nobili, A. (2021). Bounds to the pull-in voltage of a MEMS/NEMS beam with surface elasticity. *Applied Mathematical Modelling*, *91*, 1211–1226.

Ramezani, A., Alasty, A., & Akbari, J. (2007). Closed-form solutions of the pull-in instability in nanocantilevers under electrostatic and intermolecular surface forces. *International Journal of Solids and Structures*, *44*, 4925–4941.

Shenoy, V. B. (2005). Atomistic calculations of elastic properties of metallic fcc crystal surfaces. *Physical Review B*, *71*, Article 094104.

Soroush, R., Koochi, A., Kazemi, A. S., Noghrehabadi, A., Haddadpour, H., & Abadyan, M. (2010). Investigating the effect of casimir and van der Waals attractions on the electrostatic pull-in instability of nano-actuators. *Physica Scripta*, *82*, Article 045801.

Wang, G. F., & Feng, X. Q. (2009). Surface effects on buckling of nanowires under uniaxial compression. *Applied Physics Letters*, *94*, Article 141913.

Yang, J., Jia, X. L., & Kitipornchai, S. (2008). Pull-in instability of nano-switches using nonlocal elasticity theory. *Journal of Physics D (Applied Physics)*, *41*, Article 035103.

Zhang, W.-M., Yan, H., Peng, Z.-K., & Meng, G. (2014). Electrostatic pull-in instability in MEMS/NEMS: A review. *Sensors and Actuators A: Physical*, *214*, 187–218.

Zhou, L. G., & Huang, H. (2004). Are surface elastically softer or stiffer? *Applied Physics Letters*, *84*, 1940–1942.